

PET imaging of fatty acid amide hydrolase in the brain: synthesis and biological evaluation of an ^{11}C -labelled URB597 analogue

Leonie wyffels^a, Giulio G. Muccioli^b, Coco N. Kapanda^c, Geoffray Labar^c, Sylvie De Bruyne^a, Filip De Vos^a, Didier M. Lambert^{c,*}

^aDepartment of Radiopharmacy, Ghent University, Harelbekestraat 72, 9000 Ghent, Belgium

^bBioanalysis and Pharmacology of Bioactive Lipids Laboratory, Louvain Drug Research Institute, Université catholique de Louvain, CHAM7230, B-1200, Brussels, Belgium

^cUnité de Chimie Pharmaceutique et de Radiopharmacie, Louvain Drug Research Institute, Université catholique de Louvain, UCL-CMFA 73-40, B-1200 Brussels, Belgium

Received 12 January 2010; received in revised form 25 March 2010; accepted 28 March 2010

Abstract

Introduction: Fatty acid amide hydrolase (FAAH) is part of the endocannabinoid system (ECS) and has been linked to the aetiology of several neurological and neuropsychiatric disorders. So far no useful PET or SPECT tracer for in vivo visualisation of FAAH has been reported. We synthesized and evaluated a carbon-11-labeled URB597 analogue, biphenyl-3-yl [^{11}C]-4-methoxyphenylcarbamate or [^{11}C]-**1**, as potential FAAH imaging agent.

Methods: The inhibitory activity of **1** was determined in vitro using recombinant FAAH. Radiosynthesis of [^{11}C]-**1** was performed by methylation using [^{11}C]- CH_3I , followed by HPLC purification. Biological evaluation was done by biodistribution studies in wild-type and FAAH knock-out mice, and by ex vivo and in vivo metabolite analysis. The influence of URB597 pretreatment on the metabolisation profile was assessed.

Results: [^{11}C]-**1** was obtained in good yields and high radiochemical purity. Biodistribution studies revealed high brain uptake in wild-type and FAAH knock-out mice, but no retention of radioactivity could be demonstrated. Metabolite analysis and URB597 pretreatment confirmed the non-FAAH-mediated metabolisation of [^{11}C]-**1**. The inhibition mechanism was determined to be reversible. In addition, the inhibition of URB597 appeared slowly reversible.

Conclusions: Although [^{11}C]-**1** inhibits FAAH in vitro and displays high brain uptake, the inhibition mechanism seems to deviate from the proposed carbamylation mechanism. Consequently, it does not covalently bind to FAAH and will not be useful for mapping the enzyme in vivo. However, it represents a potential starting point for the development of in vivo FAAH imaging tools.

© 2010 Published by Elsevier Inc.

Keywords: Fatty acid amide hydrolase; Carbon-11; PET; URB597; Endocannabinoid system

1. Introduction

The endocannabinoid system (ECS) is a neuromodulatory system in the brain that comprises cannabinoid receptors CB_1 and CB_2 , endogenous ligands termed endocannabinoids like anandamide (AEA), transporters and several synthesizing and degrading enzymes [1,2]. Fatty acid amide hydrolase (FAAH), an integral membrane-bound enzyme, is one of the

main enzymes of the ECS. A key role of FAAH in hydrolyzing AEA was first reported in 1993 where it was called an ‘anandamide amidase’ enzyme [3]. Studies in FAAH knock-out ($\text{FAAH}^{-/-}$) mice confirmed the primary role of FAAH in controlling endogenous AEA levels in the brain and, consequently, its importance as a regulatory enzyme for key physiological functions [4]. It is thus conceivable that disease-associated changes in tissue concentration of endocannabinoids in part reflect corresponding changes in their inactivation and therefore an up- or down-regulation of FAAH. Research on the role of FAAH in pathological conditions is rising, and accumulating

* Corresponding author. Tel.: +32 2 764 50 45; fax: +32 2 764 50 35.
E-mail address: didier.lambert@uclouvain.be (D.M. Lambert).

data suggest that the symptoms of several neurological and neuropsychiatric disorders could be caused by changes in the endocannabinoid biosynthesis and degradation. Indeed, a naturally occurring single nucleotide polymorphism (SNP) in the human FAAH gene C385A (cytosine 385→adenosine) was found to be strongly associated with street drug use and problem drug/alcohol use [5]. A direct role for FAAH in the regulation of alcohol consumption was also demonstrated in a study on FAAH knock-out mice [6–9]. Furthermore, FAAH knock-out mice have reduced anxiety-like behaviour, as revealed by two different behavioural models [10]. Also, pharmacological inhibition of FAAH elicits anxiolytic-like and antidepressant-like effects in rodents [11–14], indicating a critical role played by the ECS in the pathophysiology of depression and anxiety, as well as the potential usefulness of inhibiting the enzyme. Nevertheless, the therapeutic potential of the ECS and more specifically FAAH has yet to be fully determined, and the number of disorders that may be treated will likely continue to grow.

The availability of a positron emission tomography (PET) or single photon emission computed tomography (SPECT) tracer for in vivo evaluation of FAAH in the brain would be of great interest to elucidate the specific role of the enzyme in those neurological and neuropsychiatric disorders and would greatly improve the knowledge on their aetiology. Mapping FAAH in the brain by means of a PET or SPECT tracer would stimulate the research for novel therapeutic strategies and would be useful for the evaluation of efficacy of potential FAAH inhibitors applicable in the treatment of FAAH-related disorders like anxiety and depression. In general, two approaches are being applied for characterisation of enzymes using PET or SPECT. A first approach is based on the design of radioactive substrate analogues and on the principle of metabolic trapping. This principle implies trapping of the radiolabelled hydrolysis products of the radiotracer in the tissue where the enzyme is present. The distribution of radioactivity in the brain thus reflects the distribution of the enzyme as well as its functionality [15]. A second approach is the use of a radiolabelled inhibitor for the enzyme of interest. The selective binding of the radiolabelled inhibitor to the enzyme will reflect the regional distribution of the enzyme

within the brain [16]. Several radioligands based on either of the two approaches have been developed for in vivo evaluation of enzymes like acetylcholinesterase [17–22] and the monoamine oxidases MAO-A [23,24] and MAO-B [25–27] in the human brain by PET or SPECT. To our knowledge, so far no radioligands for PET or SPECT exist for the in vivo visualisation of FAAH in the brain [28,29].

The high lipophilicity associated with the fatty acid chain present in all up-to-now known endogenous and synthetic FAAH substrates increases the risk of nonspecific binding and rapid metabolic turnover of the tracers [30,31] and thus limits the use of the principle of metabolic trapping in the development of FAAH tracers. Therefore, we chose to focus on the development of a radiolabelled FAAH inhibitor for in vivo mapping of the enzyme in the brain. Since FAAH is a member of the class of serine hydrolases, it is susceptible to inhibition by most classical serine hydrolase-directed inhibitors, including fluorophosphonates, trifluoromethyl ketones, α -keto heterocycles and carbamates [32]. The last class includes the potent and selective *O*-aryl carbamate URB597 (cyclohexylcarbamic acid 3'-carbamoylbiphenyl-3-yl ester) (Fig. 1), which has a nanomolar affinity for FAAH (44 nM in our hands, using recombinant human FAAH) and is devoid of CB₁ cannabinoid receptor affinity [33]. URB597 is reported to inhibit FAAH by an irreversible, substrate-like inhibition mechanism proposed to involve carbamylation of the catalytic nucleophile Ser²⁴¹, with the *O*-biaryl group serving as the leaving group [34,35]. Based on the structure of URB597, we synthesized analogues while focusing on the prospect of possible labelling with carbon-11 or fluorine-18. In the present study, we describe the synthesis, in vitro and in vivo evaluation of biphenyl-3-yl [¹¹C]-4-methoxyphenyl-carbamate ([¹¹C]-1) as PET tracer for in vivo visualisation of FAAH in the brain. The proposed mechanism for visualisation of FAAH using [¹¹C]-1 is based on carbamylation of the catalytic nucleophile of FAAH by the inhibitor, similar to the proposed inhibitory mechanism of URB597. This carbamylation of the Ser²⁴¹ would leave the ¹¹C-methoxyanilino group bound to the enzyme and thus provide an opportunity for mapping the enzyme in distinct brain regions using PET (Fig. 2).

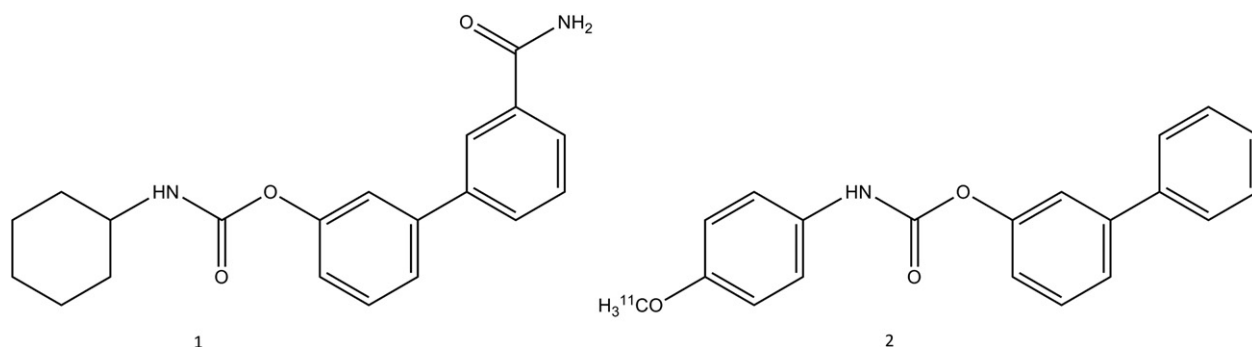


Fig. 1. Chemical structures of carbamate FAAH inhibitors URB597 (1) and [¹¹C]-1 (2).

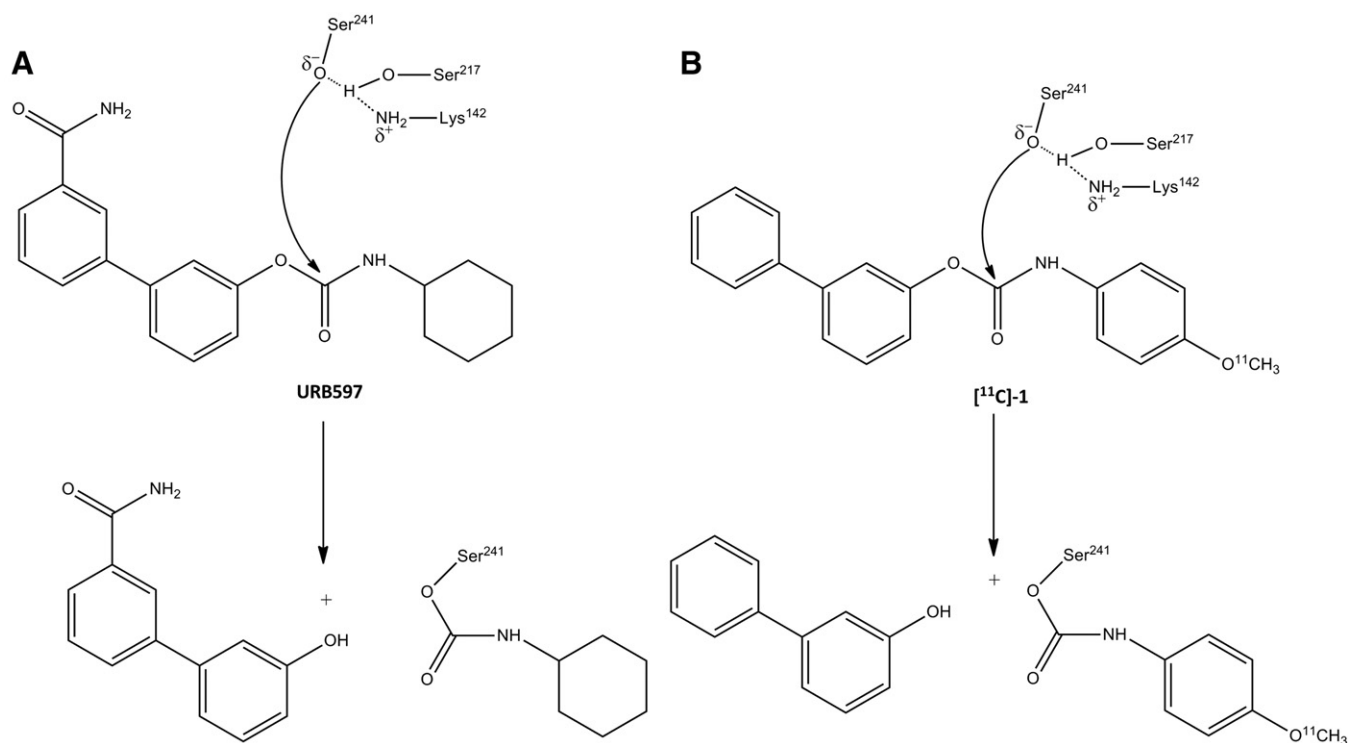


Fig. 2. Proposed mechanism for FAAH inhibition by URB597 as demonstrated by [34] (A) and hypothesized mechanism for PET visualization of FAAH using $[^{11}\text{C}]\text{-1}$ (B).

2. Materials and methods

2.1. Synthesis of compounds

All chemical reagents were obtained from commercial sources (Sigma-Aldrich Fluka, Acros Organics, Belgium) and used without further purification. Solvents used were of high-performance liquid chromatography (HPLC) grade and were purchased from ChemLab (Belgium). Nuclear magnetic resonance (^1H NMR, ^{13}C NMR) spectra were recorded on a Bruker Avance 400-MHz Ultrashield. Chemical shifts (δ) are reported relative to the tetramethylsilane peak set at 0 ppm. In the case of multiplets, the signals are reported as intervals. Signals are abbreviated as s, singlet; d, doublet; t, triplet; q, quartet; m, multiplet. Coupling constants are expressed in Hertz. MS analysis was obtained using a LCQ Advantage instrument from ThermoFisher in the APCI positive mode. Compound purity was assessed by HPLC-MS using a Supelcosil LC18 column (3 μM , 4 \times 150 mm) and a gradient of ACN and ACN–H₂O (87:13) as mobile phase. Detection was carried out in the APCI mode using a LCQ advantage mass spectrometer.

2.1.1. Biphenyl-3-yl-4-methoxyphenylcarbamate(1)

The carbamate derivative was synthesized as reported by Tarzia et al. [36]. Briefly, triethylamine (0.12 mmol) and 4-methoxyphenyl isocyanate (2.2 mmol) were added to a stirred solution of 3-phenylphenol (2 mmol) in toluene (12 ml). The reactants were kept under reflux for 14 h. The

mixture was then cooled and concentrated. Purification of the residue was done by column chromatography with cyclohexane–ethyl acetate (85:15) as eluent. The pure product was recrystallized from ethanol. Yield 85%. ^1H NMR (DMSO- d_6) δ (ppm) 10.08 (s, 1 H), 7.70–6.92 (m, 13 H), 3.72 (s, 3 H). ^{13}C NMR (DMSO- d_6) δ (ppm) 155.15, 151.83, 151.18, 141.56, 139.18, 131.59, 129.88, 127.79, 126.64, 123.59, 122.37, 120.94, 120.07, 114.06, 55.15. MS (APCI): 319 $[\text{M}]^+$.

2.1.2. Biphenyl-3-yl-4-hydroxyphenylcarbamate(2)

To a solution of biphenyl-3-yl-4-methoxyphenylcarbamate (2.8 mmol), at 0°C, in dry methylene chloride (37.5 ml), boron tribromide (581 μl , 6.1 mmol) is added using a syringe. The solution is left at room temperature overnight under stirring. Then, the solvent is evaporated under reduced pressure and the residue is resuspended in water and filtered off [38]. The solid obtained is crystallized from ethanol to yield 96% of biphenyl-3-yl-4-hydroxyphenylcarbamate. ^1H NMR (DMSO- d_6) δ (ppm) 10.02 (s, 1 H), 7.70–6.72 (m, 13 H), 5.77 (s, 1 H). ^{13}C NMR (DMSO- d_6) δ (ppm) 151.81, 151.24, 141.52, 139.19, 129.99, 129.86, 128.97, 127.79, 126.74, 123.51, 120.92, 120.37, 120.10, 115.25. MS (APCI): 306 $[\text{M}+\text{H}]^+$.

2.2. Radiosynthesis of $[^{11}\text{C}]\text{-1}$

The labelling of compound 1 with carbon-11 was carried out using a method previously described by our group [29].

Briefly, the radiotracer was prepared by radiomethylation of the corresponding desmethylprecursor **2** using [^{11}C]- CH_3I . The final product was purified by reversed phase semi-preparative HPLC (Grace Discovery Econosphere C_{18} column, 250×10 mm, particle size $10 \mu\text{m}$ +Grace Discovery Econosphere C_{18} guard 33×7 mm, particle size $10 \mu\text{m}$, eluted with $\text{MeCN}/\text{H}_2\text{O}/\text{HCOOH}$ (65:35:0.1, v/v) at a flow rate of 4 ml/min). The radioactive peak corresponding to [^{11}C]-**1** ($t_{\text{R}}=9$ min) was collected and diluted with Dulbecco's Phosphate Buffered Saline [DPBS, 0.0095M (PO_4), pH 7.4, 45 ml]. The mixture was passed over a C_{18} cartridge (Alltech Maxi-Clean SPE Prevail C_{18} , previously activated with ethanol and water). The cartridge was rinsed with water (10 ml) and the radiolabelled compound was eluted with ethanol (1 ml).

Specific radioactivity (GBq/ μmol) was determined with analytical HPLC (GraceSmart RP 18 column, 250×4.6 mm, particle size $5 \mu\text{m}$) calibrated for absorbance ($\lambda=254$ nm) response per mass of ligand. The radioactivity of the radioligand peak (decay corrected) (GBq) was divided by the mass of the associated carrier peak (μmol). For biological evaluation, the purified radioligand was diluted with saline reducing the ethanol concentration to 10%.

2.3. Quality control

An aliquot of [^{11}C]-**1** was co-injected with $1 \mu\text{g}$ of **1** into the HPLC system [GraceSmart RP 18 column, 250×4.6 mm, particle size $5 \mu\text{m}$, eluted with $\text{MeCN}/\text{H}_2\text{O}/\text{HCOOH}$ (60:40:0.1 v/v) as mobile phase] to confirm its identity. Eluate was monitored with an absorbance detector ($\lambda=254$ nm) in series with a Ludlum 220 scaler ratemeter equipped with a GM probe for radiation detection. With this system, the retention time for [^{11}C]-**1** is 12.2 min.

2.4. Partition coefficient determination

The partition coefficient of [^{11}C]-**1** was measured according to the 'shake-flask' method [37]. Approximately $10 \mu\text{l}$ of [^{11}C]-carba5 (2–4 MBq) was added to a test tube containing *n*-octanol (3 ml) and DPBS [0.0095M (PO_4), pH 7.4, 3 ml]. The mixture was shaken manually for 3 min, vortexed for 1 min at room temperature and then centrifuged (4000 rpm, 3 min). After separation of layers, a 0.5-ml aliquot of both layers was taken and counted for radioactivity in a Packard Cobra automated γ -counter, back correcting for decay (Cobra Autogamma, five 1×1 -in. NaI(Tl) crystals, Packard Canberra). The aqueous layer was discarded, and 2.5 ml of fresh DPBS was added. The mixture was shaken manually for 3 min, vortexed for 1 min and centrifuged (4000 rpm, 3 min), and a 0.5-ml aliquot of both layers was counted for radioactivity. This process was repeated once more. The partition coefficients were calculated: $D = \text{counts in } n\text{-octanol}/\text{counts in DPBS}$. Reported $\log D$ value represents the mean of three determinations and is expressed as $\text{mean} \pm \text{S.D.}$

2.5. In vitro evaluation

2.5.1. FAAH Inhibition assay

The assay was performed as previously described using recombinant human FAAH fused to maltose binding protein (hFAAH) [38,39]. Briefly, hFAAH was diluted to the appropriate assay protein concentration ($6 \mu\text{g}$ per assay) in Tris-HCl buffer (10 mM, pH 7.6) containing 1 mM EDTA. Aliquots ($165 \mu\text{l}$) were added to glass tubes containing $10 \mu\text{l}$ of test compound. Blanks contained assay buffer instead of hFAAH. [^3H]-AEA ($25 \mu\text{l}$, final concentration $2 \mu\text{M}$, containing $50 \times 10^{-3} \mu\text{Ci}$ of $60 \text{ Ci}/\text{mmol}$ [^3H]-AEA) was added to the test tubes, and the samples were incubated for 10 min at 37°C . After the incubation the reaction was stopped by adding $400 \mu\text{l}$ chloroform/methanol (1:1, v/v), followed by vortex mixing and centrifugation (5 min, 2500 rpm) for phase separation. Aliquots ($200 \mu\text{l}$) of the methanol/buffer phase containing the water soluble reaction products (containing [^3H]-ethanolamine) were measured for tritium content by liquid scintillation spectroscopy with quench correction. Experiments were performed in threefold. Radiolabelled arachidonylethanolamide ([^3H]-AEA, labelled on its ethanolamine moiety, specific activity of $60 \text{ Ci}/\text{mmol}$) was obtained from American Radiolabeled Chemicals, Inc. (St Louis, MO, USA). Nonradioactive AEA was purchased from Cayman Chemical Company (Ann Arbor, MI, USA). Fatty acid-free bovine serum albumin (BSA) was obtained from Sigma (Belgium).

2.5.2. Reversibility study

The reversibility of hFAAH inactivation by inhibitors was assessed by rapid dilution. In a total volume of $100 \mu\text{l}$, hFAAH ($182 \mu\text{g}$) was incubated at room temperature for 1 h with compound **1** ($20 \mu\text{M}$), URB597 ($10 \mu\text{M}$), CAY10402 (60 nM) or MAFP (400 nM). DMSO was used for the controls. The applied inhibitor concentrations were at least 20-fold the IC_{50} value and gave 85–90% inhibition of [^3H]-AEA hydrolysis before dilution. After the preincubation, an aliquot ($40 \mu\text{l}$) of the enzyme-inhibitor mixture was diluted 100-fold into the FAAH assay buffer [Tris-HCl buffer (10 mM, pH 7.6) containing 1 mM EDTA]. The diluted mixture was vortexed and left to stand at room temperature. Thirty minutes and 90 min postdilution, an aliquot ($175 \mu\text{l}$) of the diluted mixture was taken and [^3H]-AEA ($25 \mu\text{l}$, final concentration $2 \mu\text{M}$, containing $50 \times 10^{-3} \mu\text{Ci}$ of $60 \text{ Ci}/\text{mmol}$ [^3H]-AEA) was added to the test tubes, and the samples were incubated for 30 min at 37°C . Sample workup was performed as described under the FAAH Inhibition Assay section 2.5.1. Experiments were performed in threefold. Positive control values were obtained by incubation of the inhibitors at concentrations corresponding to the 100-fold diluted concentrations. The samples were incubated for 30 min at 37°C followed by sample workup as described for the FAAH inhibition assay.

URB597, CAY10402 and MAFP were obtained from Cayman.

2.5.3. Brain homogenate preparation

Fresh dissected C57BL/6J mice or FAAH^{-/-} brain was homogenized in PBS using a glass homogenizer and subsequently centrifuged at 4°C for 20 min at 18,000×g. The pellet was resuspended in PBS and centrifuged again at 4°C for 20 min at 18,000×g. The latter operation was performed twice. The resulting pellet was resuspended in buffer (10 mM Tris–HCl, 1 mM EDTA). Protein content of the preparation was determined according to the method of Bradford, using bovine serum albumin as standard, and aliquots were stored at –80°C until used for assay.

2.5.4. In vitro metabolite analysis

Ten microliters of [¹¹C]-1 (370–740 kBq) was incubated with C57BL/6J or FAAH^{-/-} brain homogenates (400–700 µg protein/assay) or with recombinant FAAH (80 µg) in Tris–HCl buffer (10 mM, pH 7.6) containing 1 mM EDTA and 0.1% BSA (final volume of 500 µl) at 37°C for 30 min with shaking. The reaction was stopped by adding 500 µl cold MeCN, followed by vortex and centrifugation (2 min, 6000 rpm) to remove the proteins. Five hundred microliters of supernatant was injected into the HPLC system for analysis [Grace Discovery Econosphere C18 column, 250×10 mm, particle size 10 µm+Grace Discovery Econosphere C18 guard 33×7 mm, particle size 10 µm, using MeCN/H₂O/HCOOH (65:35:0.1, v/v) as the mobile phase at a flow rate of 4 ml/min]. The HPLC eluate was collected in fractions of 30 s, and the radioactivity was counted with an automated γ-counter. For the FAAH inhibition assay, brain homogenates or recombinant FAAH was preincubated for 10 min with 3 mM URB597 (Cayman) in Tris–HCl buffer (10 mM, pH 7.6) containing 1 mM EDTA and 0.1% BSA (final volume of 500 µl) at 37°C with shaking. Next, [¹¹C]-1 was added and the mixture was incubated for another 30 min at 37°C and analyzed as described above. All experiments were performed in triplicate.

2.6. In vivo evaluation

2.6.1. Biodistribution study

A biodistribution study of [¹¹C]-1 was performed in male C57BL/6J weighing 20–23 g (Charles River Laboratories, Belgium) and in male FAAH knock-out mice weighing 20–23 g. FAAH knock-out (FAAH^{-/-}) mice were kindly provided by The Scripps Research Institute (La Jolla, CA, USA). All animal experiments were conducted according to the regulations of the Belgian law and the Ghent University local ethics committee (ECP 08/33). Mice were immobilized in a restraining device and injected in a tail vein with approximately 3.7 MBq of [¹¹C]-1 dissolved in 200 µl ethanol/saline (1:9). At 1, 10, 30 or 60 min postinjection (*n*=3 for each time point), mice were sacrificed by cervical dislocation under isoflurane anesthesia. Blood was collected and the brain and main organs to be examined were rapidly removed and weighed. Radioactivity in the dissected organs and blood was measured using an automatic γ-counter. Aliquots of the injected tracer solution (*n*=5) were weighed

and counted for radioactivity (Packard Cobra automated γ-counter equipped with five 1×1-in. NaI(Tl) crystals) to determine the injected radioactivity dose received by the animals. The results were corrected for decay, and the uptake of radioactivity in blood and organs was expressed as percentage of the injected dose per gram of tissue plus or minus the standard deviation (%ID/g±S.D.).

2.6.2. Plasma and brain metabolites

In vivo metabolism of the tracers was studied in C57BL/6J mice and in FAAH^{-/-}. Mice (*n*=3 for each time point) were injected in a tail vein with 18–37 MBq of tracer dissolved in 200 µl ethanol/saline (1:9). At 1, 10 or 30 min postinjection, mice were sacrificed by cervical dislocation under isoflurane anesthesia. Blood was collected in a vacuum tube (containing 3.6 mg K₃EDTA; Vacutest Kima, Italy) and the brain was rapidly removed. Blood samples were centrifuged at 4000×g for 3 min, and plasma was isolated. Plasma (200 µl) was mixed with MeCN (800 µl), and the mixture was vortexed for 30 s, followed by centrifugation for 3 min at 4000×g. The supernatant (500 µl) was analyzed by HPLC. The brain was transferred to a tube and homogenized with MeCN (1 ml). The mixture was vortexed for 30 s and centrifuged for 3 min at 4000×g. The supernatant (500 µl) was analyzed on HPLC. A Grace Discovery Econosphere C18 column (250×10 mm; 10 µm particle size) coupled to a Grace Discovery Econosphere C18 guard (33×7 mm, particle size 10 µm) was used. The mobile phase was MeCN/H₂O/HCOOH (65:35:0.1 v/v) at a flow rate of 4 ml/min. The HPLC eluate was collected in fractions of 30 s and their radioactivity was counted with an automated γ-counter.

To validate the above-described extraction procedure, control experiments (*n*=3) were done using the blood and brain of untreated mice. Two hundred microliters of plasma and brain was spiked with 1 MBq authentic tracer. Sample workup was identical as described above. After centrifugation, the pellet and supernatant were separated and counted for radioactivity in an automated γ-camera. Extraction efficiencies were expressed as percentage of radioactivity present in the supernatant compared to the total amount of radioactivity present in the brain or plasma sample. The stability of the tracer during the workup was determined by analysis of the supernatant of spiked plasma and brain samples using the same HPLC system as described above.

2.6.3. URB597 pretreatment assay

The influence of FAAH inhibition on the in vivo metabolite profile of [¹¹C]-1 was studied in C57BL/6J mice. The FAAH inhibitor URB597 was dissolved in DMSO and sonicated for a few minutes. DPBS was added to obtain an injectable solution (DMSO/DPBS, 1:1). Mice (*n*=3 for each treatment strategy) were injected intraperitoneally (ip) with URB597 (0.5 mg/kg body weight or 3 mg/kg body weight). Sixty minutes after URB597 injection (0.5 mg/kg or 3 mg/kg body weight) or 120 min after URB597 injection

(3 mg/kg body weight), the mice were injected in a tail vein with 18–37 MBq of [^{11}C]-**1** dissolved in 200 μl ethanol/saline (1:9). At 30 min postinjection, mice were sacrificed by cervical dislocation under isoflurane anesthesia. Blood was collected and the brain was dissected and processed as described above. Supernatant (500 μl) of processed plasma and brain was analyzed on HPLC using a Grace Discovery Econosphere C18 column (250 \times 10 mm; 10 μm particle size) coupled to a Grace Discovery Econosphere C18 guard (33 \times 7 mm, particle size 10 μm) and MeCN/H $_2$ O/HCOOH (65:35:0.1 v/v) as mobile phase at a flow rate of 4 ml min. HPLC eluate fractions of 30 s were collected and measured for radioactivity in an automated γ -counter.

2.7. Analysis of data

For the FAAH inhibition assay, the pooled data expressed as percentage of control activity containing the same carrier concentration were analyzed using the built-in equation “sigmoidal dose-response (variable slope)” of the GraphPad Prism computer program (GraphPad Software, Inc., San Diego, CA, USA). For the reversibility study, the obtained results were normalized against positive control values. The significance of the differences obtained was assessed by one-way ANOVA test (followed by Dunnett post-test).

The metabolite data are expressed as mean percentage of the total activity \pm S.D. The Student's *t* test was used to evaluate significant differences. *P* value < .05 was considered significantly different.

3. Results

3.1. FAAH Inhibition assay

The FAAH inhibitory action of compound **1** was assessed by its ability to prevent the enzyme from hydrolyzing anandamide tritiated in the ethanolamine part (^3H)-AEA). Experiments were performed using 10 concentrations of test compound **1** in the range of 1 mM–1 nM. With this assay, **1** was determined to inhibit the hydrolysis of ^3H -AEA by hFAAH with an IC_{50} value of 436 nM. An IC_{50} value of 40 nM was obtained for URB597 when tested in the same assay.

3.2. Radiosynthesis of [^{11}C]-**1**, quality control and partition coefficient determination

[^{11}C]-**1** was synthesized by carbon-11 methylation of the desmethyl precursor biphenyl-3-yl 4-hydroxyphenylcarbamate using [^{11}C]-CH $_3$ I under basic conditions. With optimized reaction conditions of 3 μmol desmethylprecursor, 250 μl DMF and 10 μl NaH (1M) in a 10-min reaction at 30 $^\circ\text{C}$, [^{11}C]-**1** was obtained in an average decay-corrected radiochemical yield of 35 \pm 9% ($n=7$) (based on [^{11}C]-CH $_3$ I trapped in a reaction vial). Overall radiosynthesis time from end-of-bombardment till end of synthesis, including HPLC purification, was about 40 min. [^{11}C]-**1** was obtained with a

specific activity of 376 \pm 135 GBq/ μmol ($n=7$) at EOS and with a radiochemical purity >99%. Product identity was confirmed by coelution with reference compound **1** after coinjection on HPLC.

The partition coefficient *D* of [^{11}C]-**1** was determined by the shake-flask method and calculated as $D = \text{counts in } n\text{-octanol} / \text{counts in PBS}$. A log*D* value of 2.27 \pm 0.07 ($n=3$) was obtained.

3.3. Biodistribution study in wild-type and FAAH knock-out mice

Biodistribution and brain uptake of [^{11}C]-**1** were assessed in male C57BL/6J mice as well as in FAAH $^{-/-}$ mice. C57BL/6J mice were chosen as this strain was the background of the FAAH $^{-/-}$ mice [4]. The distribution of ^{11}C radioactivity in selected organs of the mice at 1, 10, 30 and 60 min after the injection of [^{11}C]-**1** is presented in Fig. 3. The distribution of [^{11}C]-**1** in wild-type and FAAH $^{-/-}$ mice was highly similar. The tracer displayed a high initial brain uptake of 8.6 \pm 2.3 %ID/g in wild-type mice and 8.3 \pm 0.2 %ID/g in FAAH $^{-/-}$ mice at 1 min postinjection, followed by a continuous decrease until the end of the study. At 60 min postinjection, brain uptake of 0.6 \pm 0.2 %ID/g in wild-type mice and 0.7 \pm 0.2 %ID/g in FAAH $^{-/-}$ mice was still present in the brain. At 90 min post-injection, brain uptake of 0.4 \pm 0.1 %ID/g in wild-type mice and 0.7 \pm 0.2 %ID/g in FAAH $^{-/-}$ mice was still present in the brain. No steady state in brain uptake, characteristic for binding of the labelled inhibitor to the enzyme, could be demonstrated in the brain of wild-type mice (Fig. 4). Despite the lower initial uptake of ^{11}C radioactivity in the blood (4.3 \pm 1.1 %ID/g in wild-type mice and 3.7 \pm 0.4 %ID/g in FAAH $^{-/-}$ mice at 1 min postinjection), a slower washout resulted in higher blood levels compared to brain uptake at later time points in both mouse strains. The highest %ID/g was detected in metabolising tissues and in well-vascularised tissues like the lungs and the heart. In wild-type mice, radioactivity uptake peaked in heart, lungs, liver and kidneys during the first minute after tracer injection and then subsequently declined. Uptake in liver decreased from 8.8 \pm 4.2 %ID/g at 1 min postinjection to 3.0 \pm 0.2 %ID/g at 90 min postinjection, whereas in small intestine, the highest uptake was reached at 30 min postinjection (6.7 \pm 1.5 %ID/g) and slowly declined to 5.3 \pm 2.1 %ID/g at 90 min postinjection. In liver, kidneys and small intestine of FAAH $^{-/-}$ mice, a lower radioactivity uptake was detected compared to wild-type mice, even though this difference failed to reach a statistical significance. This difference was most clear at 1 and 10 min postinjection. Highest uptake in the liver of FAAH $^{-/-}$ mice was seen at 10 min postinjection (4.6 \pm 1.4 %ID/g) and the uptake remained rather constant throughout the study. In the kidneys and small intestines, highest uptake was detected at 1 min postinjection (6.7 \pm 3.4 %ID/g) and at 90 min postinjection (6.2 \pm 1.3 %ID/g), respectively. Although the continuous clearance of radioactivity from the liver and kidneys seen in wild-type mice was less pronounced in

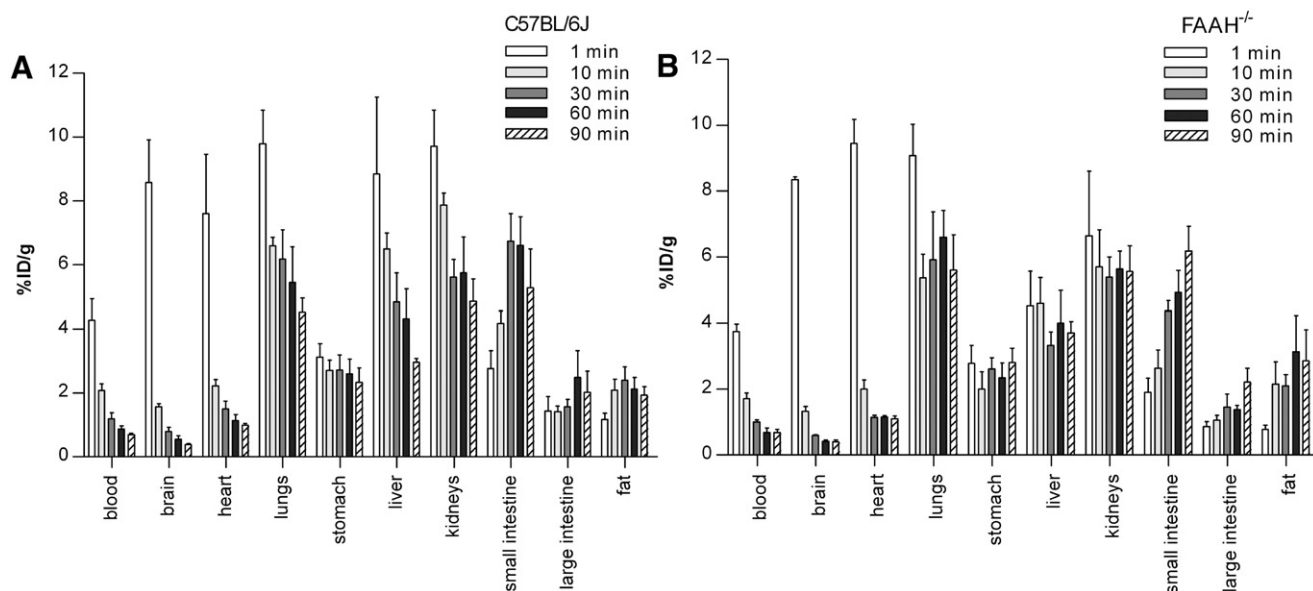


Fig. 3. Uptake (%ID/g) of radioactivity in selected mice organs [C57BL/6J mice (A) or FAAH^{-/-} mice (B)] at various time points after intravenous injection of [¹¹C]-1.

FAAH^{-/-} mice, these uptake profiles suggest hepatobiliary and urinary clearance of the tracer in both mouse strains.

3.4. In vitro metabolism assay

Based on the assumption that **1** will inhibit FAAH by the same carbamylation mechanism as proposed for URB597, we expected metabolism of the tracer by FAAH and subsequent covalent binding of the ¹¹C-labeled methoxyanilino leaving group to the enzyme and thus retention of radioactivity in the brain. However, no retention of radioactivity in the brain of wild-type mice compared to the brain of FAAH^{-/-} mice could be demonstrated in the biodistribution study. Therefore, an

ex vivo metabolite analysis was performed using recombinant FAAH and wild-type or FAAH^{-/-} brain homogenates to study the metabolism of [¹¹C]-1 by FAAH. Following incubation of [¹¹C]-1 with C57BL/6J or FAAH^{-/-} brain homogenates for 30 min at 37°C, only intact tracer could be detected after HPLC analysis of supernatant. Pre-incubation of brain homogenates with the potent and selective FAAH inhibitor URB597 prior to the addition of [¹¹C]-1 had no influence on the metabolism profile. Incubation of the tracer with recombinant FAAH resulted in the same metabolite profile with only intact tracer and no metabolites formed. These results indicate that, although the structure of **1** resembles that of URB597, the mechanism of FAAH inhibition by **1** seems to deviate from the URB597 proposed mechanism of inhibition.

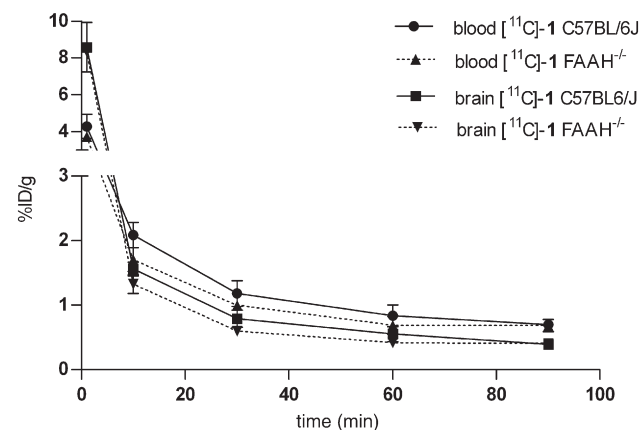


Fig. 4. Time dependency of uptake (%ID/g) of [¹¹C] radioactivity in the blood and brain of C57BL/6J mice or FAAH^{-/-} mice after intravenous injection of [¹¹C]-1.

3.5. Plasma and brain metabolite analysis

The in vivo metabolism profile of [¹¹C]-1 was studied in plasma and brain of wild-type as well as FAAH^{-/-} mice. Validation experiments with spiked blood and brain revealed an extraction efficiency for [¹¹C]-1 of 95±1% for plasma and 87±3% for brain samples. HPLC analysis of the spiked samples demonstrated no degradation of the tracer during the extraction procedure. In vivo metabolism of [¹¹C]-1 was examined 1, 10 and 30 min postinjection. The results are presented in Table 1. In the plasma of both C57BL/6J and FAAH^{-/-} mice, [¹¹C]-1 is rapidly metabolised with only 8.4±1.4% intact tracer left in C57BL/6J mice and 11±3.0% in FAAH^{-/-} mice at 10 min and no unmetabolised tracer left 30 min postinjection. Only one polar metabolite with a retention time of 3.5 min is formed in the plasma of both C57BL/6J mice and FAAH^{-/-}. The same polar metabolite

Table 1

Metabolite profile in C57BL/6J and FAAH^{-/-} mice at 1, 10 and 30 min after intravenous injection of [¹¹C]-1

	Tissue	Time (min)	Retention time on HPLC (min)		
			3.5	5–8	11**
C57BL/6J	Brain	1	0.4±0.1		98±0.2
		10	23±3.8	5.4±1.3	71±5.0
		30	57±6.6	12±3.0	31±9.1
	Plasma	1	21±3.3		75±3.6
		10	86±2.4		8.4±1.4
		30	100		0
FAAH ^{-/-}	Brain	1	0.4±0.04		98±0.4
		10	19±2.5	5.0±0.2	76±2.2
		30	35±4.8*	10±2.5	55±4.4*
	Plasma	1	13±1.0*		86±1.5*
		10	87±1.8		11±3.0
		30	96±7.0		3.0±5.0

Values are expressed as percent of total activity±S.D. (*n*=3).

* Significantly different (*P*<.05) from C57BL/6J mice.

** Parent compound: [¹¹C]-1.

also appears in the brain of both mouse strains. Between a retention time of 5 and 8 min, additional polar metabolites can be detected in the brain of C57BL/6J and FAAH^{-/-} mice at 10 min postinjection (together 5.4±1.3% in C57BL/6J mice and 5.0±0.2% in FAAH^{-/-}) and 30 min postinjection (together 12±3.0% in C57BL/6J mice and 10±2.5% in FAAH^{-/-} mice). Although the metabolite profile looks essentially the same in C57BL/6J and FAAH^{-/-} mice, at 30 min post tracer injection, metabolite amounts of [¹¹C]-1 in brain were statistically different in FAAH^{-/-} compared to C57BL/6J mice. The strong resemblance of the metabolite profile of [¹¹C]-1 in C57BL/6J mice to the profile in FAAH^{-/-} points to a non-FAAH-mediated metabolism of the tracer in vivo.

3.6. Metabolite analysis in wild-type mice pretreated with URB597

To confirm that the in vivo metabolism of [¹¹C]-1 indeed is not FAAH mediated, the influence of FAAH inhibition by URB597 on the in vivo metabolite profile in C57BL/6J mice was studied. In case the metabolism of the tracer is FAAH mediated, pretreatment of mice with URB597 should influence the metabolite profile, while no changes should be detected if FAAH is not involved in the metabolism of [¹¹C]-1. As according to the pharmacological profile of URB597, FAAH inhibition is rapid in onset (<15 min) and persistent (>12 h) following intraperitoneal injection of 0.3 mg/kg URB597 in rats [40], we chose in a first experiment to administer a dose of 0.5 mg/kg ip 1 h prior to tracer injection. Radiolabelled metabolites were determined in plasma and brain samples 30 min after tracer injection using reversed-phase HPLC. No statistically significant differences in metabolite amounts could be detected after pretreatment of the mice with URB597 in a dose of 0.5 mg/kg ip, 1 h prior to tracer injection (Table 2). Raising the URB597 dose to 3 mg/kg ip [12] did not result in a

Table 2

Metabolite profile in C57BL/6J mice 30 min after intravenous injection of [¹¹C]-1 following pretreatment with URB597

URB597 administration	Tissue	Retention time on HPLC (min)		
		3.5	5–8	11
No URB597 administration	Brain	57±6.6	12±3.0	31±9.1
	Plasma	100		0
0.5 mg/kg 1 h prior to tracer	Brain	54±3.6	16±0.2	35±5.7
	Plasma	98±4.1		1.7±2.9
3 mg/kg 1 h prior to tracer	Brain	54±1.6	14±3.4	31±4.1
	Plasma	100		0
3 mg/kg 2 h prior to tracer	Brain	58±0.5	15±6.0	27±5.7
	Plasma	100		0

Values are expressed as percent of total activity±S.D. (*n*=3).

statistically significantly different metabolite profile either, nor did a longer waiting period (2 h) between URB597 injection and tracer injection.

3.7. Reversibility study

Because these results raised the question of the type of interaction between 1 and FAAH, we assessed whether compound 1 acted as a reversible or irreversible hFAAH inhibitor, by performing a rapid dilution experiment. The known reversible FAAH inhibitor CAY10402 and the known irreversible FAAH inhibitor MAFP were also tested in the same assay. As the biodistribution experiments and metabolite assays suggest that compound 1 does not inhibit FAAH by the proposed irreversible carbamylation mechanism, we also tested the template URB597 (Fig. 5).

In this assay, CAY10402 displayed a statistically significant recovery of activity 30 and 90 min postdilution, indicating a reversible inhibition mechanism. In contrast, MAFP-treated FAAH did not recover activity, even 90 min after dilution, as FAAH activity was not statistically

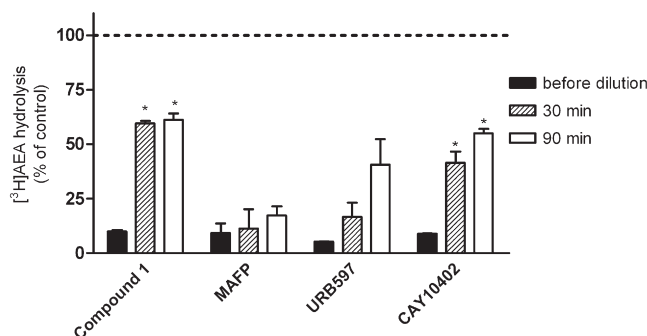


Fig. 5. Reversibility of FAAH inactivation by 1 (20 μM), URB597 (10 μM), CAY10402 (60 nM) and MAFP (400 nM). Enzyme activity was measured at the indicated time points after 100-fold dilution of the enzyme–inhibitor complex. The data represent the means and S.E.M. from three independent experiments performed in duplicate. **P*<.05 compared to no-dilution condition.

significantly different from that in the nondiluted samples. In contrast, inhibition of FAAH by compound **1** was reversible as the dilution allowed for the recovery of FAAH activity. Note that for URB597-treated FAAH a slow recovery of the activity was observed postdilution.

4. Discussion and conclusions

Increasing evidence suggests a pivotal role of FAAH in several neurological and neuropsychiatric disorders. Studies in FAAH knock-out mice and the finding of a SNP in the human FAAH gene linked FAAH with addiction. Also, the observation that genetic or pharmacological inactivation of FAAH results in anxiolytic [13] and antidepressant [11,41] phenotypes in rodents suggests that FAAH may play an important therapeutic target for these and possibly many other CNS disorders. The exact picture of the involvement of FAAH in those disorders is yet to be clarified and the availability of a PET tracer aimed at visualizing the enzyme in the brain in vivo would greatly help in this matter. Visualisation of brain FAAH in vivo could cast light on possible disease-associated up- or down-regulations of the enzyme and would help to evaluate the efficacy of potential therapeutic FAAH inhibitors. Since no useful PET or SPECT tracer for the in vivo visualisation of FAAH has been reported so far, the aim of this study was the synthesis and in vivo evaluation of a radiolabelled URB597 analogue, [^{11}C]-4-methoxyphenylcarbamate ([^{11}C]-**1**), as potential PET tracer for in vivo evaluation of FAAH in the brain. Carbamate FAAH inhibitors, represented by URB597, are particularly efficacious in vivo, possibly due to the proposed irreversible mechanism of action, analogous to the inactivation of acetylcholinesterase by commercial carbamate drugs (e.g., pyridostigmine, rivastigmine) for the treatment of Alzheimer's disease [34]. By incubation of purified recombinant FAAH with URB597 followed by tryptic digestion and MALDI-TOF mass spectrometry analysis, Alexander and Cravatt [34] provided evidence that carbamates inactivate FAAH by carbamylation of Ser²⁴¹ with the *O*-biaryl group serving as the leaving group (Fig. 2). These results confirmed the findings of Basso et al. [35], who protonated several carbamates by electrospray ionisation and found that lability of the C(O)–O bond correlated with their potency of FAAH inhibition, suggesting the role of the phenolic fragment as leaving group. Since a variety of moieties are accepted as *N*-substituents [42] and the biphenyl moiety was suggested to be a key parameter in orienting these inhibitors inside the catalytic site, we decided, in the design of a radiolabelled URB597 analogue, to retain the biphenyl moiety and replace the cyclohexyl by a methoxy-anilino group, providing an opportunity for labelling with ^{11}C and thus the possibility of using [^{11}C]-**1** for visualisation of FAAH in vivo. Carbamylation of the serine nucleophile and the consequent binding of the ^{11}C -labelled methoxyanilino leaving group to the enzyme would provide an

opportunity for mapping the enzyme in distinct brain regions using PET.

An in vitro assay using recombinant human FAAH and [^3H]-AEA as substrate revealed that **1** inhibits FAAH activity with an IC₅₀ value of 436 nM. Although this affinity is, to some extent, lower than the high target affinity shown by most tracers, we still decided to further evaluate the ex vivo and in vivo behaviour of the radiolabelled compound because both human and rat FAAH enzymes, likewise cannabinoid receptors, are expressed at high levels in the central nervous system [43–45], thus somewhat relaxing the affinity requirement [46]. In addition, numerous pathologies are characterized by altered levels of FAAH expression. This was found for instance in Alzheimer's disease where FAAH expression is up-regulated [47,48], or in animal models of depression where FAAH activity was increased [49]. Moreover, URB597, the lead compound for [^{11}C]-**1**, is particularly efficacious in vivo, displaying activity in rodent models of inflammatory and neuropathic pain as well as anxiety and depression [50], and is the topic of numerous studies. The study of the in vivo behaviour of a radiolabelled analogue of this leading carbamate FAAH inhibitor could, in our opinion, make a valuable contribution to the knowledge on this class of FAAH inhibitors and be helpful in the research for and discovery of a useful FAAH imaging agent.

Biodistribution studies were performed in C57BL/6J mice as well as in FAAH^{-/-} mice. A difference in retention of radioactivity in the brain between the two mouse strains was expected based on the hypothesized carbamylation of FAAH by the tracer in C57BL/6J mice and subsequent release of the ^{11}C -methoxyaniline. However, the uptake profile of [^{11}C]-**1** in the blood and brain of FAAH^{-/-} mice resembled the uptake in the blood and brain of C57BL/6J mice. In both mouse strains, the tracer showed, as we expected by the obtained log*D* value of 2.27, a very high initial brain uptake, followed, however, by a continuous washout. The lack of retention of radioactivity in the brain is likely due to the too low affinity of our compound for the enzyme. Yet because we expected nevertheless retention of radioactivity in the brain, we questioned the irreversibility of the inhibition mechanism. In ex vivo metabolisation studies, using recombinant FAAH and C57BL/6J and FAAH^{-/-} brain homogenates, no metabolisation of the tracer was observed. Contrasting with this, the in vivo metabolism studies revealed the formation of a polar metabolite in the brain and plasma of both C57BL/6J and FAAH^{-/-} mice. As this metabolite is present in the plasma at 1 min postinjection and appears in the brain only at later time points, it is possible that it is formed in the periphery and has the ability to cross the blood–brain barrier and thus to appear in the brain. FAAH^{-/-} mice differ from wild-type mice in that a significantly higher amount of intact tracer was present in the brain, 30 min post tracer injection in FAAH^{-/-} mice. However, since the metabolite profiles essentially looked the same in both mouse strains and since pretreatment of

C57BL/6J mice with URB597 prior to tracer injection did not influence the metabolite profile, the higher metabolisation rate in C57BL/6J brain is probably not FAAH dependent. A possible explanation is that other enzyme systems, which are less active in the FAAH^{-/-} mice, are responsible for the tracer breakdown. Considering that FAAH is a member of the serine hydrolase superfamily, with more than 200 members in the human proteome, achieving selectivity in FAAH inhibition is challenging [51,52]. Interaction of [¹¹C]-1 with liver carboxylesterases could result in the formation of the observed radiolabelled polar metabolite. Note that it is highly likely that this polar metabolite is [¹¹C]-*p*-methoxyaniline since *p*-methoxyaniline, when injected in the same HPLC system as used for the metabolite analysis, elutes at the same retention time as the polar metabolite.

Based on the ex vivo and in vivo metabolite profile, we can conclude that [¹¹C]-1 does not inhibit FAAH by the same carbamylation mechanism as proposed for URB597 and, consequently, does not covalently bind to the enzyme. The rapid dilution experiment showed recovery of activity, confirming a reversible inhibition mechanism. It should be mentioned that, in our hand and quite surprisingly, URB597 displayed a slowly reversible inhibition mechanism in this assay, rather than the expected irreversible inhibition mechanism. This is in contrast to the results of Ahn et al. [50] who showed a negligible recovery of FAAH activity with URB597 in a similar rapid dilution assay.

We can conclude that despite successful labelling with ¹¹C and a high brain uptake, [¹¹C]-1 will not be useful for in vivo visualisation of cerebral FAAH due to a lack of retention of radioactivity in the brain. Although we hypothesized that high expression of FAAH in the brain could relax the affinity requirement, the affinity of compound 1 appears to be too low after all, resulting in a lack of retention of radioactivity in the brain. Still, the need for a reliable tracer for in vivo visualisation of cerebral FAAH is great and thus further research should be dedicated to the development of labelled FAAH inhibitors. Conceptually, compound 1 is a reasonable starting place for the design of labelled enzyme inhibitors for in vivo mapping of cerebral FAAH. Other URB597 analogues should be synthesized with a higher affinity for the enzyme and a closer resemblance to the original structure in order to favour the carbamylation inhibition mechanism. Alternatively, potent and selective FAAH inhibitors distinct from URB597, like the recently developed piperidine urea FAAH inhibitors [50], can be used as a template.

Acknowledgment

The authors sincerely wish to thank Maarten Dhaenens for the protein content determination. The authors especially thank Johan Sambre for his excellent technical assistance. We are grateful to Dr. Benjamin F. Cravatt for providing the FAAH knock-out mice.

References

- [1] De Petrocellis L, Cascio MG, Di Marzo V. The endocannabinoid system: a general view and latest additions. *Br J Pharm* 2004;141:765–74.
- [2] Lambert DM, Fowler CJ. The endocannabinoid system: drug targets, lead compounds, and potential therapeutic applications. *J Med Chem* 2005;48:5059–87.
- [3] Deutsch DG, Chin SA. Enzymatic-synthesis and degradation of anandamide, a cannabinoid receptor agonist. *Biochem Pharmacol* 1993;46:91–796.
- [4] Cravatt BF, Demarest K, Patricelli MP, Bracey MH, Giang DK, Martin BR, et al. Supersensitivity to anandamide and enhanced endogenous cannabinoid signaling in mice lacking fatty acid amide hydrolase. *Proc Natl Acad Sci U S A* 2001;98:9371–6.
- [5] Sipe JC, Chiang K, Gerber AL, Beutler E, Cravatt BF. A missense mutation in human fatty acid amide hydrolase associated with problem drug use. *Proc Natl Acad Sci U S A* 2002;99:8394–9.
- [6] Basavarajappa BS, Yalamanchili R, Cravatt BF, Cooper TB, Hungund BL. Increased ethanol consumption and preference and decreased ethanol sensitivity in female FAAH knockout mice. *Neuropharmacology* 2006;50:834–44.
- [7] Blednov YA, Cravatt BF, Boehm SL, Walker D, Harris RA. Role of endocannabinoids in alcohol consumption and intoxication: studies of mice lacking fatty acid amide hydrolase. *Neuropsychopharmacology* 2007;32:1570–82.
- [8] Vinod KY, Sanguino E, Yalamanchili R, Manzanares J, Hungund BL. Manipulation of fatty acid amide hydrolase functional activity alters sensitivity and dependence to ethanol. *J Neurochem* 2008;104:233–43.
- [9] Hansson AC, Bermudez-Silvaz FJ, Hyytia P, Sanchez-Vera I, Rimondini R, de Fonseca FR, et al. Genetic impairment of frontocortical endocannabinoid degradation and high alcohol preference. *Neuropsychopharmacology* 2007;32:117–26.
- [10] Moreira FA, Kaiser N, Monory K, Lutz B. Reduced anxiety-like behaviour induced by genetic and pharmacological inhibition of the endocannabinoid-degrading enzyme fatty acid amide hydrolase (FAAH) is mediated by CB1 receptors. *Neuropharmacology* 2008;54:141–50.
- [11] Gobbi B, Bambico FR, Mangieri R, Bortolato M, Campolongo P, Solinas M, et al. Anti-depressant like activity and modulation of brain monoaminergic transmission by blockade of anandamide hydrolysis. *Proc Natl Acad Sci* 2005;102(51):18620–5.
- [12] Bortolato M, Mangieri RA, Fu J, Kim JH, Arguello O, Duranti A, et al. Antidepressant-like activity of the fatty acid amide hydrolase inhibitor URB597 in a rat model of chronic mild stress. *Biol Psychiatry* 2007;62(10):1103.
- [13] Kathuria S, Gaetani S, Fegley D, Valino F, Duranti A, Tontini A, et al. Modulation of anxiety through blockade of anandamide hydrolysis. *Nature Med* 2003;9:76–81.
- [14] Naderi N, Haghparast A, Saber-Tehrani A, Rezaei N, Alizadeh AM, Khani A, et al. Interaction between cannabinoid compounds and diazepam on anxiety-like behaviour of mice. *Pharmacol Biochem Behav* 2008;89:64–75.
- [15] Namba H, Fukushi K, Nagatsuka S, Iyo M, Shinotoh H, Tanada S, et al. Positron emission tomography: quantitative measurement of brain acetylcholinesterase activity using radiolabeled substrates. *Methods* 2002;27:242–50.
- [16] Kikuchi T, Okamura T, Fukushi K, Takahashi K, Toyohara J, Okada M, et al. Cerebral acetylcholinesterase imaging: development of the radioprobes. *Curr Top Med Chem* 2007;7:1790–9.
- [17] Tavitian B, Pappata S, Planas AM, Jobert A, Bonnotlours S, Crouzel C, et al. In vivo visualisation of acetylcholinesterase with positron emission tomography. *NeuroReport* 1993;4:535–8.
- [18] Musachio JL, Flesher JE, Scheffel UA, Rauseo P, Hilton J, Mathews WB, et al. Radiosynthesis and mouse brain distribution studies of [¹¹C]-1 CP-126,998: a PET ligand for in vivo study of acetylcholinesterase. *Nuc Med Biol* 2002;29:547–52.

- [19] Irie T, Fukushi K, Akimoto Y, Tamagami H, Nozaki T. Design and evaluation of radioactive acetylcholine analogs for mapping brain acetylcholinesterase (Ache) in-vivo. *Nuc Med Biol* 1994;21:801–8.
- [20] Namba H, Irie T, Fukushi K, Iyo M. In-vivo measurement of acetylcholinesterase activity in the brain with a radioactive acetylcholine analog. *Brain Res* 1994;667:278–82.
- [21] Ueda T, Irie T, Fukushi K, Namba H, Iyo M, Takatoku K, et al. Synthesis of [¹²³I]N-methyl-3-(2-hydroxy-5-iodopen-4-enyl)-4-acetoxypiperidine. An acetylcholine analogue. Symposium abstract, XIIth International Symposium on Radiopharmaceutical Chemistry, Uppsala, Sweden; 1997.
- [22] Kikuchi T, Zhang MR, Ikota N, Fukushi K, Okamura T, Suzuki K, et al. N-[F-18]fluoroethylpiperidin-4ylmethyl acetate, a novel lipophilic acetylcholine analogue for PET measurement of brain acetylcholinesterase activity. *J Med Chem* 2005;48:2577–83.
- [23] Dolle F, Valette H, Bramouille Y, Guenther I, Fuseau C, Coulon C, et al. Synthesis and in vivo imaging properties of [C-11]befloxatone: a novel highly potent positron emission tomography ligand for mono-amine oxidase-A. *Bioorg Med Chem Lett* 2003;13:1771–5.
- [24] Bergstrom M, Westerberg G, Langstrom B. C-11-Harmine as a tracer for monoamine oxidase A (MAO-A): in vitro and in vivo studies. *Nuc Med Biol* 1997;24:287–93.
- [25] Bench CJ, Price GW, Lammertsma AA, Cremer JC, Luthra SK, Turton D, et al. Measurement of human cerebral monoamine-oxidase type-B (Mao-B) activity with positron emission tomography (Pet) — a dose ranging study with the reversible inhibitor Ro-19-6327. *Eur J Clin Pharmacol* 1991;40:169–73.
- [26] Lammertsma AA, Bench CJ, Price GW, Cremer JE, Luthra SK, Turton D, et al. Measurement of cerebral monoamine oxidase-B activity using L-[C-11]deprenyl and dynamic positron emission tomography. *J Cereb Blood Flow Metab* 1991;11:545–56.
- [27] Freedman NMT, Mishani E, Krausz Y, Weininger J, Lester H, Blaugrund E, et al. In vivo measurement of brain monoamine oxidase B occupancy by rasagiline, using C-11- L-deprenyl and PET. *J Nuc Med* 2005;46:1618–24.
- [28] wyffels L, De Bruyne S, Blanckaert P, Lambert DM, De Vos F. Radiosynthesis, in vitro and in vivo evaluation of I-123-labeled anandamide analogues for mapping brain FAAH. *Bioorg Med Chem* 2009;17:49–56.
- [29] Wyffels L, Muccioli GG, De Bruyne S, Moerman L, Lambert DM, Sambre J, et al. Synthesis, in vitro and in vivo evaluation, and radiolabeling of aryl anandamide analogues as candidate radioligands for in vivo imaging of fatty acid amide hydrolase in the brain. *J Med Chem* 2009;52:4613–22.
- [30] Waterhouse R. Determination of lipophilicity and its use as a predictor of blood–brain barrier penetration of molecular imaging agents. *Mol Imaging Biol* 2003;5:376–89.
- [31] Pajouhesh H, Lenz GR. Medicinal chemical properties of successful central nervous system drugs. *J Am Soc Exp Therap* 2005;2:541–53.
- [32] Vandevoorde S. Overview of the chemical families of fatty acid amide hydrolase and monoacylglycerol lipase inhibitors. *Curr Top Med Chem* 2008;8:247–67.
- [33] Mor M, Rivara S, Lodola A, Plazzi PV, Tarzia G, Duranti A, et al. Cyclohexylcarbamic acid 3'- or 4'-substituted biphenyl-3-yl esters as fatty acid amide hydrolase inhibitors: synthesis, quantitative structure-activity relationships, and molecular modeling studies. *J Med Chem* 2004;47:4998–5008.
- [34] Alexander JP, Cravatt BF. Mechanism of carbamate inactivation of FAAH: implications for the design of covalent inhibitors and in vivo functional probes for enzymes. *Chem Biol* 2005;12:1179–87.
- [35] Basso E, Duranti A, Mor M, Piomelli D, Tontini A, Tarzia G, et al. Tandem mass spectrometric data-FAAH inhibitory activity relationships of some carbamic acid O-aryl esters. *J Mass Spectrom* 2004;39:1450–5.
- [36] Tarzia G, Duranti A, Gatti G, Piersanti G, Tontini A, Rivara S, et al. Synthesis and structure–activity relationships of FAAH inhibitors: cyclohexylcarbamic acid biphenyl esters with chemical modulation at the proximal phenyl ring. *Chem Med Chem* 2006;1:130–9.
- [37] Wilson A, Jin L, Garcia A, DaSilva JN, Houle S. An admonition when measuring the lipophilicity of radiotracers using counting techniques. *Appl Rad Isotopes* 2001;54:203–8.
- [38] Muccioli GG, Fazio N, Scriba GKE, Poppitz W, Cannata F, Poupaert JH, et al. Substituted 2-thioxoimidazolidin-4-ones and imidazolidine-2,4-diones as fatty acid amide hydrolase inhibitors templates. *J Med Chem* 2006;49:417–25.
- [39] Labar G, Vliet FV, Wouters J, Lambert DM. A MBP-FAAH fusion protein as a tool to produce human and rat fatty acid amide hydrolase: expression and pharmacological comparison. *Amino Acids* 2008;34:127–33.
- [40] Piomelli D, Tarzia G, Duranti A, Tontini A, Mor M, Compton TR, et al. Pharmacological profile of the selective FAAH inhibitor KDS-4103 (URB597). *CNS Drug Rev* 2006;12:21–38.
- [41] Nairu PS, Varvel SA, Ahn K, Cravatt BF, Martin BR, Lichtman AH. Evaluation of fatty acid amide hydrolase inhibition in murine models of emotionality. *Psychopharmacology* 2006;192:61–70.
- [42] Mor M, Lodola A, Rivara S, Vacondio F, Duranti A, Tontini A, et al. Synthesis and quantitative structure–activity relationship of fatty acid amide hydrolase inhibitors: modulation at the N-portion of biphenyl-3-yl alkylcarbamates. *J Med Chem* 2008;51:3487–98.
- [43] Thomas EA, Cravatt BF, Danielson PE, Gilula NB, Sutcliffe JG. Fatty acid amide hydrolase, the degradative enzyme for anandamide and oleamide, has selective distribution in neurons within the rat central nervous system. *J Neurosci Res* 1997;50:1047–52.
- [44] Egertova M, Giang DK, Cravatt BF, Elphick MR. A new perspective on cannabinoid signalling: complementary localization of fatty acid amide hydrolase and the CB1 receptor in rat brain. *Proc R Soc Lond* 1998;2085–91.
- [45] Desarnaud F, Cadas H, Piomelli D. Anandamide amidohydrolase activity in rat-brain microsomes — Identification and partial characterization. *J Biol Chem* 1995;270:6030–5.
- [46] Horti AG, Van Laere K. Development of radioligands for in vivo imaging of type 1 cannabinoid receptors (CB1) in human brain. *Curr Pharm Desig* 2008;14:3363–83.
- [47] Benito C, Nunez E, Tolon RM, Carrier EJ, Rabano A, Hillard CJ, et al. Cannabinoid CB2 receptors and fatty acid amide hydrolase are selectively overexpressed in neuritic plaque-associated glia in Alzheimer's disease brains. *J Neurosci* 2003;23:11136–41.
- [48] Nunez E, Benito C, Tolon RM, Hillard CJ, Griffin WST, Romero J. Glial expression of cannabinoid CB2 receptors and fatty acid amide hydrolase are beta amyloid-linked events in Down's syndrome. *Neurosci* 2008;151:104–10.
- [49] Reich CG, Taylor ME, McCarthya MM. Differential effects of chronic unpredictable stress on hippocampal CB1 receptors in male and female rats. *Behav Brain Res* 2009;203:264–9.
- [50] Ahn K, Johnson DS, Fitzgerald LR, Liimatta M, Arendse A, Stevenson T, et al. Novel mechanistic class of fatty acid amide hydrolase inhibitors with remarkable selectivity. *Biochem* 2007;46:13019–30.
- [51] Ahn K, Johnson DS, Mileni M, Beidler D, Long JZ, McKinney MK, et al. Discovery and characterization of a highly selective FAAH inhibitor that reduces inflammatory pain. *Chem Biol* 2009;16:411–20.
- [52] Zhang D, Saraf A, Kolasa T, Bhatia P, Zheng GZ, Patel M, et al. Fatty acid amide hydrolase inhibitors display broad selectivity and inhibit multiple carboxylesterases as off targets. *Neuropharmacology* 2007;52:1095–105.